Supporting Information

Overcoming polarization-breakdown trade-off via hydrogen bonding-modulated molecular stacking in high-temperature high-energy-density flexible dielectric

*Minhao Yang[1, 2, *], Haoran Sun[1], Junjie Wang[1], Shufan Yu[1], Zhongjun Zhou[1], Shiang Zhao[1], Huarui Yan[1], Jiajun Qu[3], Jun Liu[3, *], Bobo Tian[4,*], Zhi-Min Dang[2, *]*

[1] *Institute of Energy Power Innovation, North China Electric Power University, Beijing, 102206, China*

[2] *State Key Laboratory of Power System Operation and Control, Department of Electrical Engineering, Tsinghua University, Beijing, 100084, China*

[3] *State Key Laboratory of Organic-Inorganic Composites, Beijing University of Chemical Technology, Beijing, 100029, China*

[4] *Key Laboratory of Polar Materials and Devices, Ministry of Education, Shanghai Center of Brain-inspired Intelligent Materials and Devices, Shanghai Key Laboratory of Multidimensional Information Processing, East China Normal University, Shanghai, 200241, China*

Correspondence and requests for materials should be addressed to：

minhao.yang@ncepu.edu.cn (Prof. M. Yang); dangzm@tsinghua.edu.cn (Prof. Z. M. Dang); liujun@mail.buct.edu.cn (Prof. J. Liu); bbtian@ee.ecnu.edu.cn (Prof. B. Tian)

1. Weibull distribution of breakdown strength

The breakdown strength of PEI-based dielectrics were determined using a two-parameter Weibull statistic described as

$$P(E) = 1 - exp\left(-(E/\alpha)^{\beta}\right)$$

Where $P(E)$ is the cumulative probability of breakdown failure, E is the applied electric field, β is the scale parameter, which is the breakdown strength at a cumulative failure probability of 63.2%. The shape parameter α is the slope of the fitted Weibull curve, which represents the scattering degree of the experiment results[1, 2].

2. Hopping conduction mechanism

Hopping conduction describes the charge transport within polymer dielectrics. The thermally excited charge carriers can escape from their trap site to another via a tunneling effect.

$$J = 2qdn\nu \times exp(-\frac{E_a}{kT}) \times sinh(\frac{qdE}{2kT})$$

Where d is the average hopping distance between adjacent trap sites, n is the electron concentration in the dielectric, ν is the thermal vibration frequency of the trapped electron, and E_α is the activation energy, E is the applied electric field, q is the electron charge, k is the Boltzmann constant and T is the temperature, respectively. A shorter hopping distance usually indicates a deep trap in the dielectrics[3].

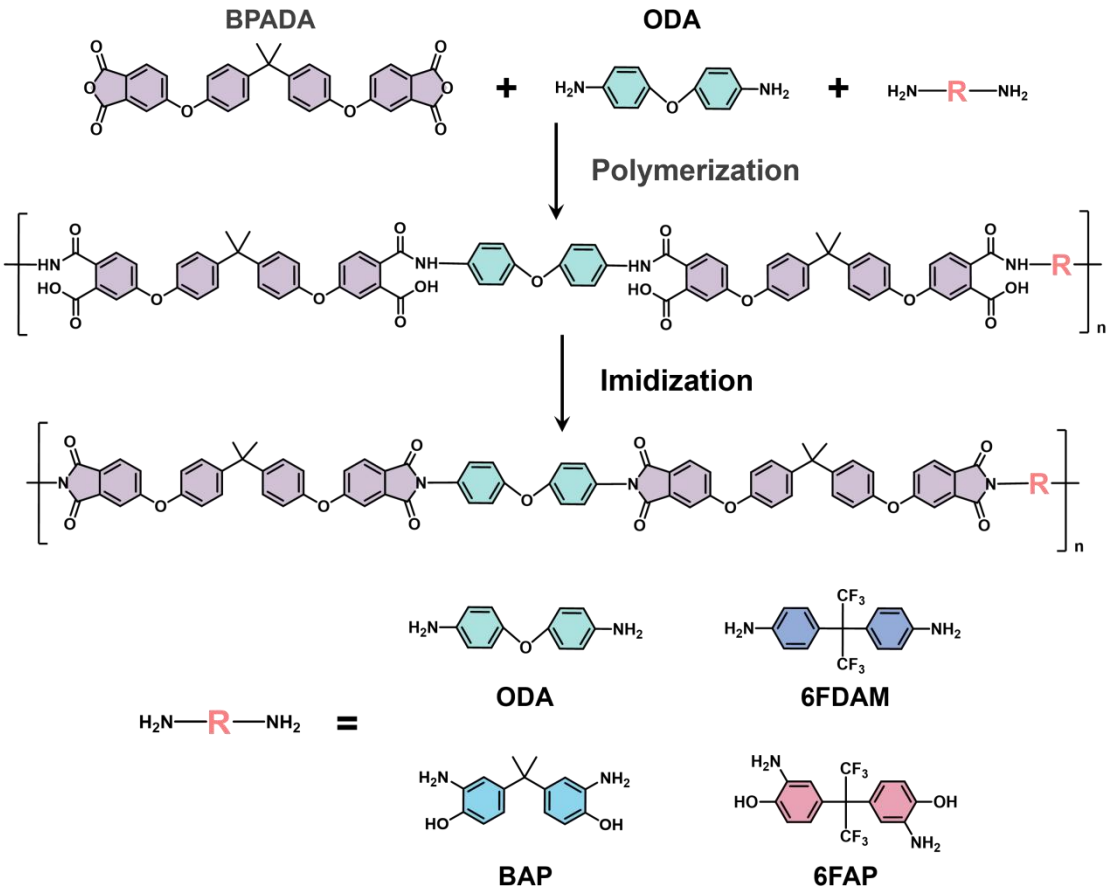

Fig. S1 Schematic illustration of the synthesis procedures of various PEI-based dielectrics.

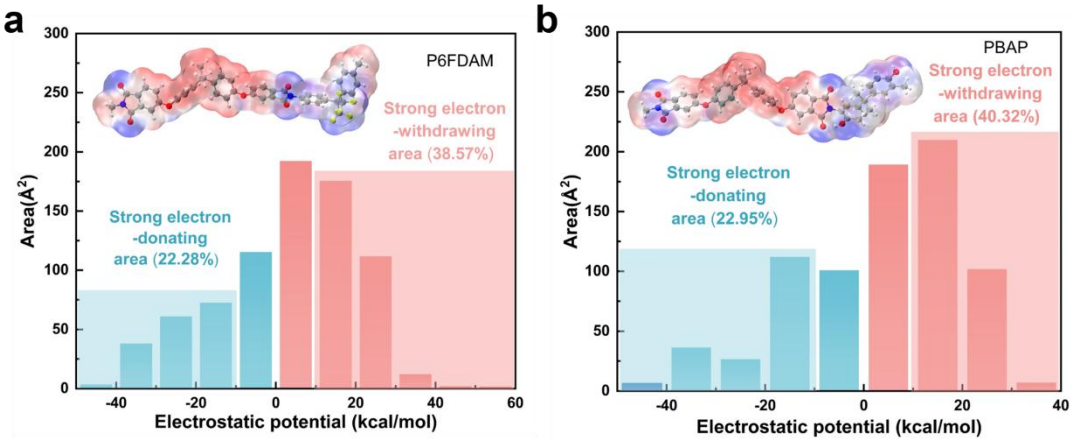

Fig. S2 ESP distribution of P6FDAM and PBAP.

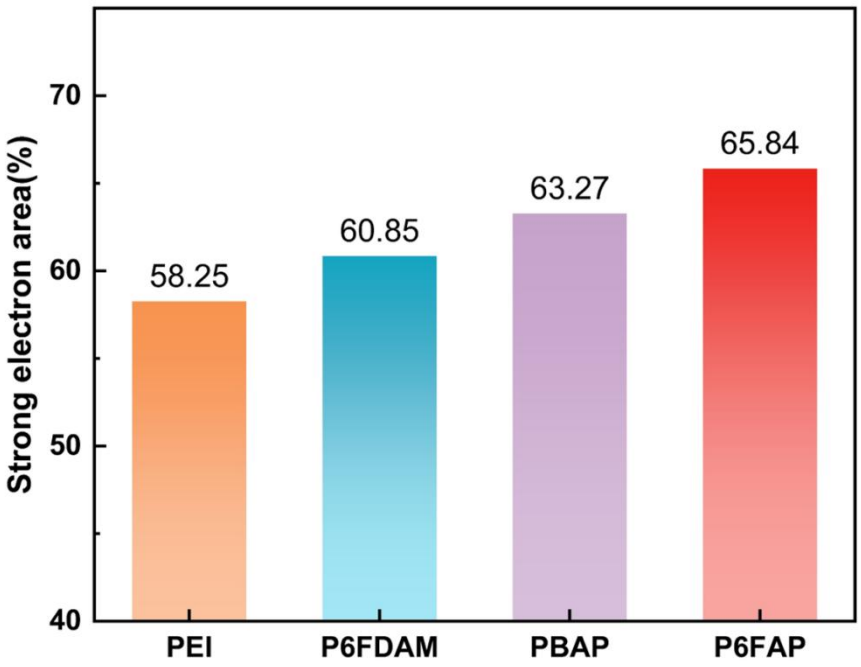

Fig. S3 Comparison of the strong electrostatic area of pristine PEI, P6FDAM, PBAP and P6FAP.

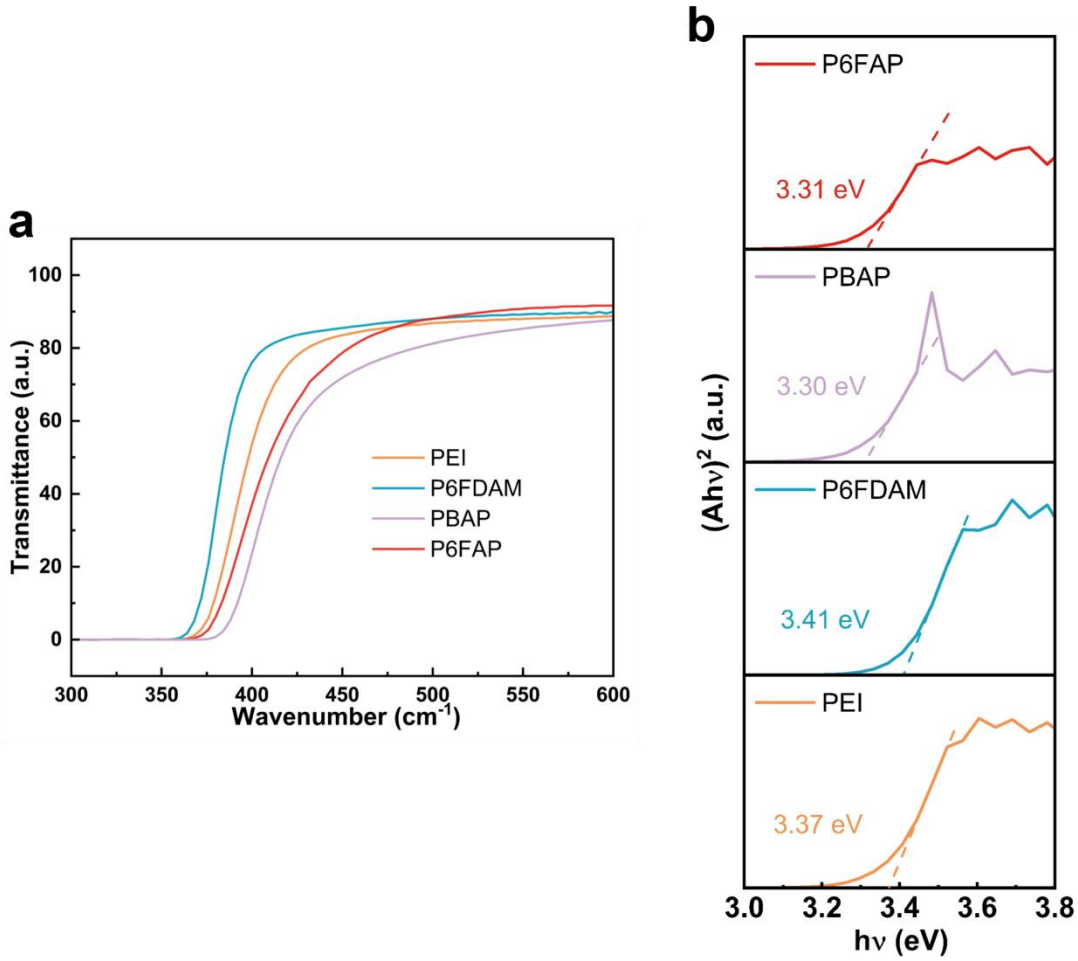

Fig. S4 a UV-vis spectra of pristine PEI, P6FDAM, PBAP and P6FAP. **b** The optical bandgap deduced from the corresponding UV-vis spectra.

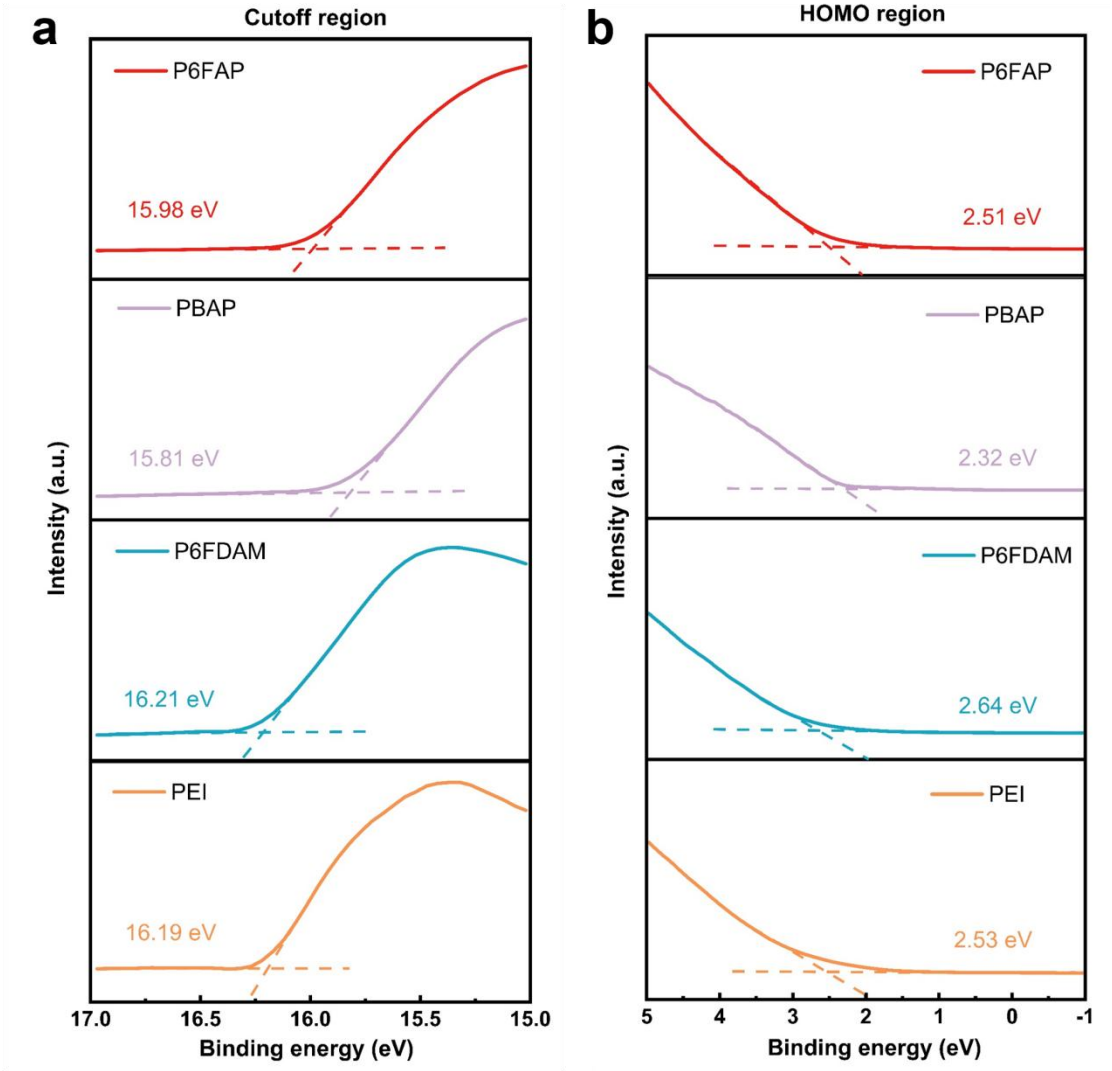

Fig. S5 UPS spectra of the **a** secondary electron cutoff region and **b** HOMO region of pristine PEI, P6FDAM, PBAP and P6FAP.

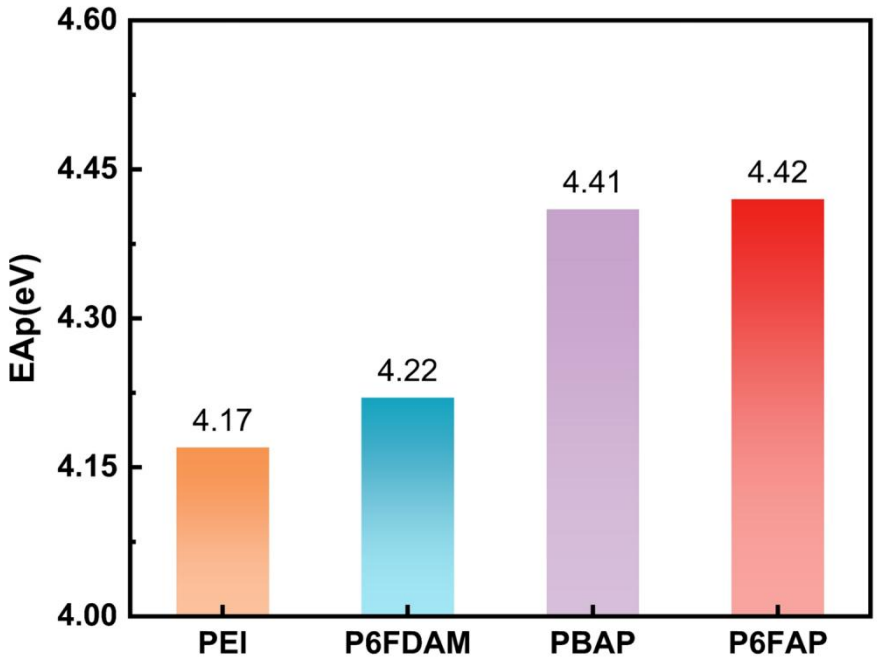

Fig. S6 Comparison of the electron affinity of pristine PEI, P6FDAM, PBAP and P6FAP.

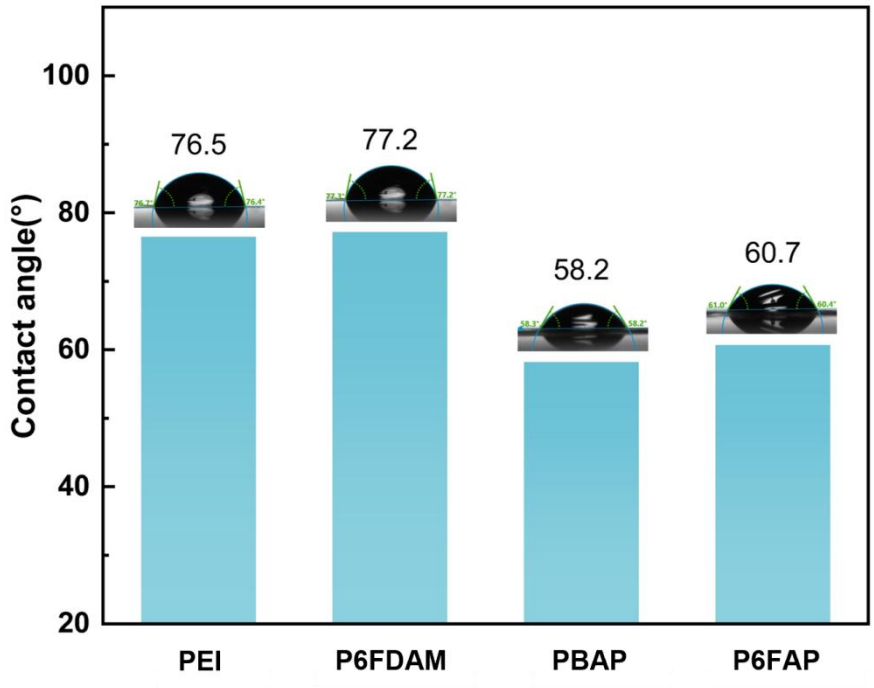

Fig. S7 Comparison of the contact angles of pristine PEI, P6FDAM, PBAP and P6FAP.

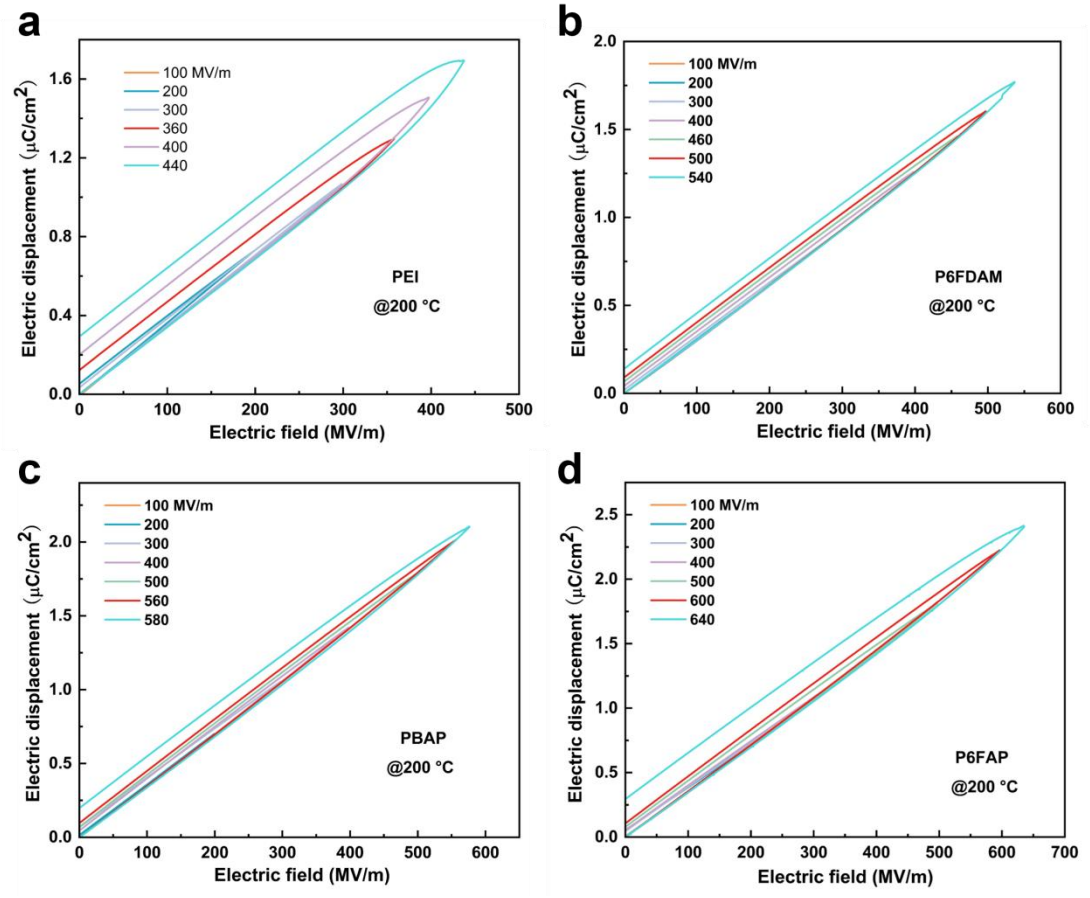

Fig. S8 Unipolar *D-E* loops of pristine PEI, P6FDAM, PBAP and P6FAP as a function of electric field at 200 °C.

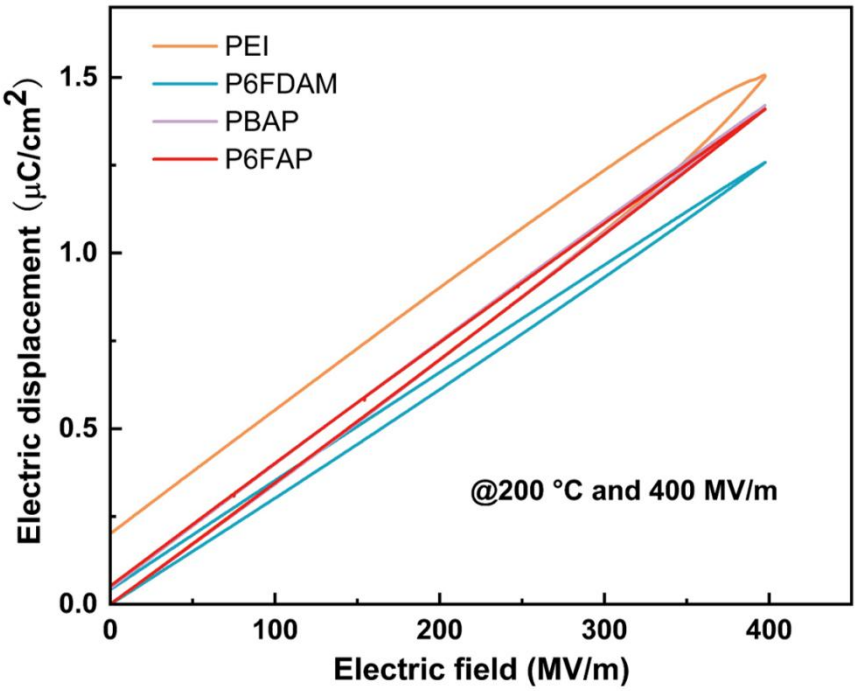

Fig. S9 Comparison of the unipolar *D-E* loops of pristine PEI, P6FDAM, PBAP and P6FAP at 200 °C and 400 MV/m.

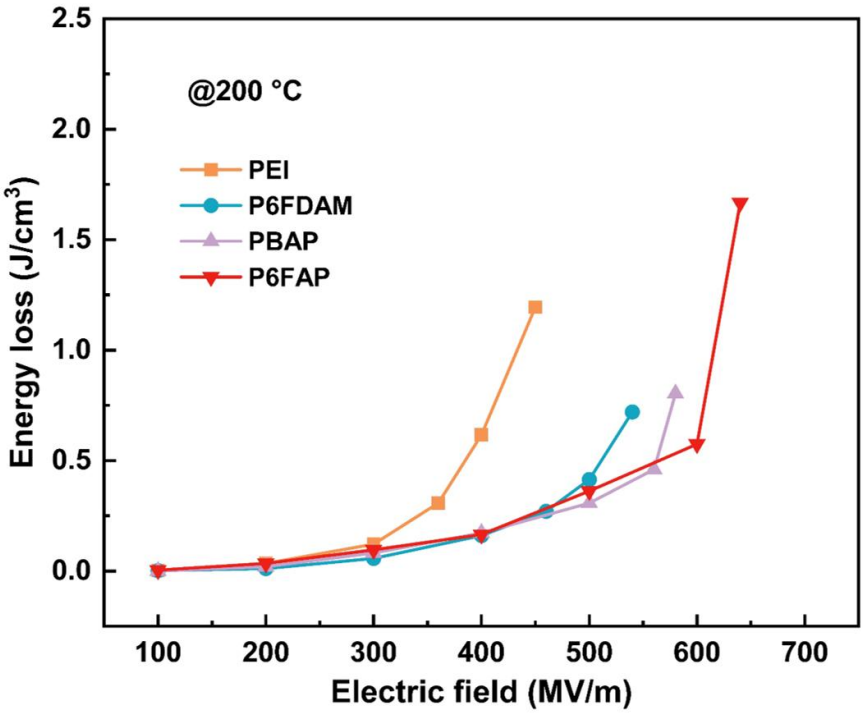

Fig. S10 Energy loss of pristine PEI, P6FDAM, PBAP and P6FAP as a function of electric field at 200 °C.

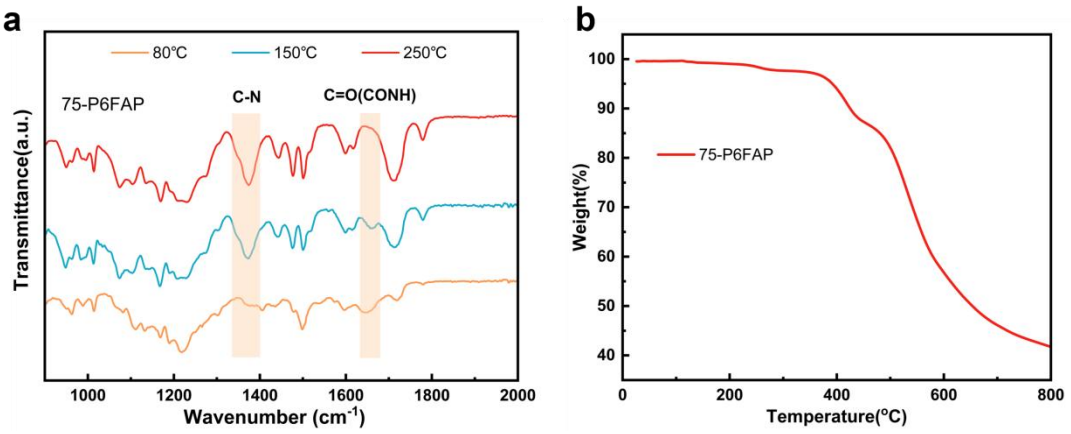

Fig. S11 a FT-IR curves of 75-P6FAP copolymer with different thermal treatment temperatures. **b** TGA curve of 75-P6FAP copolymer.

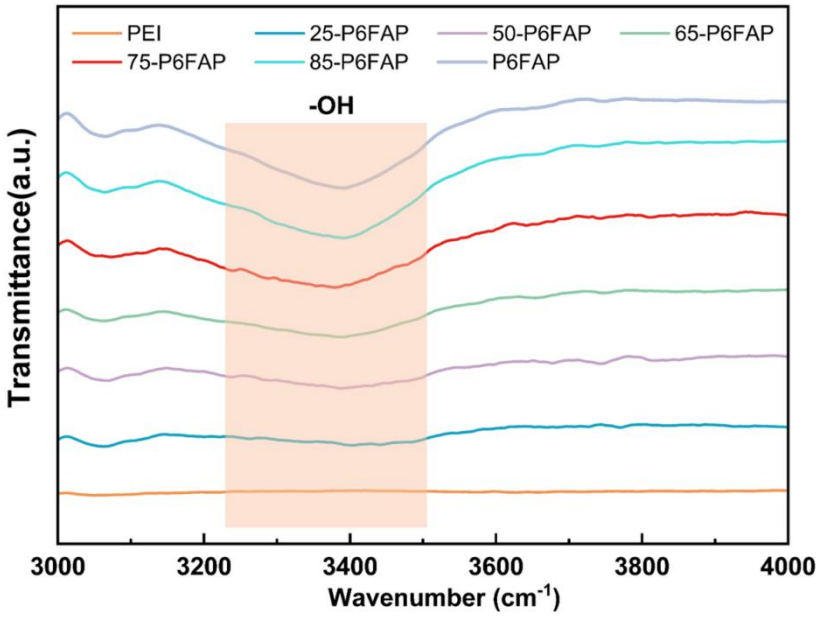

Fig. S12 Maximized FT-IR spectra of pristine PEI and P6FAP dielectrics with different mole fractions of 6FAP diamine monomer.

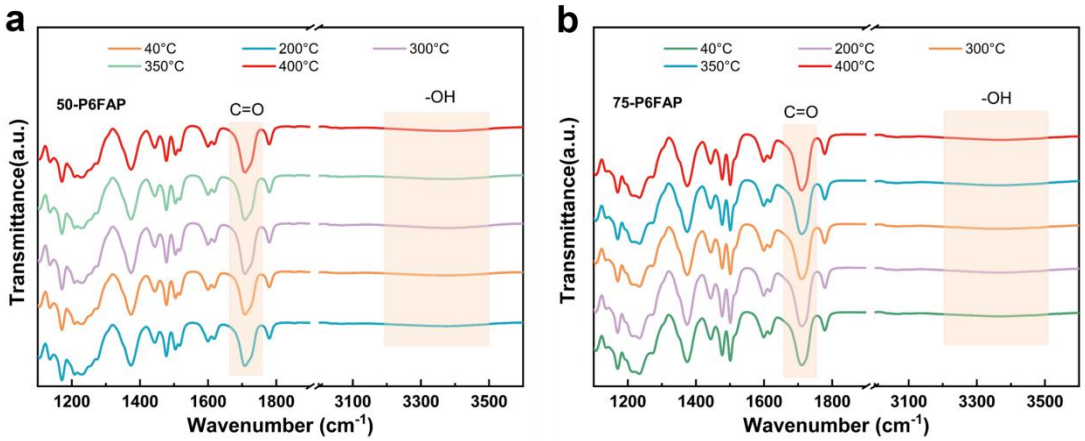

Fig. S13 VT-IR of P6FAP dielectrics with different mole fractions of 6FAP diamine monomer with temperature ranging from 40 °C to 400 °C.

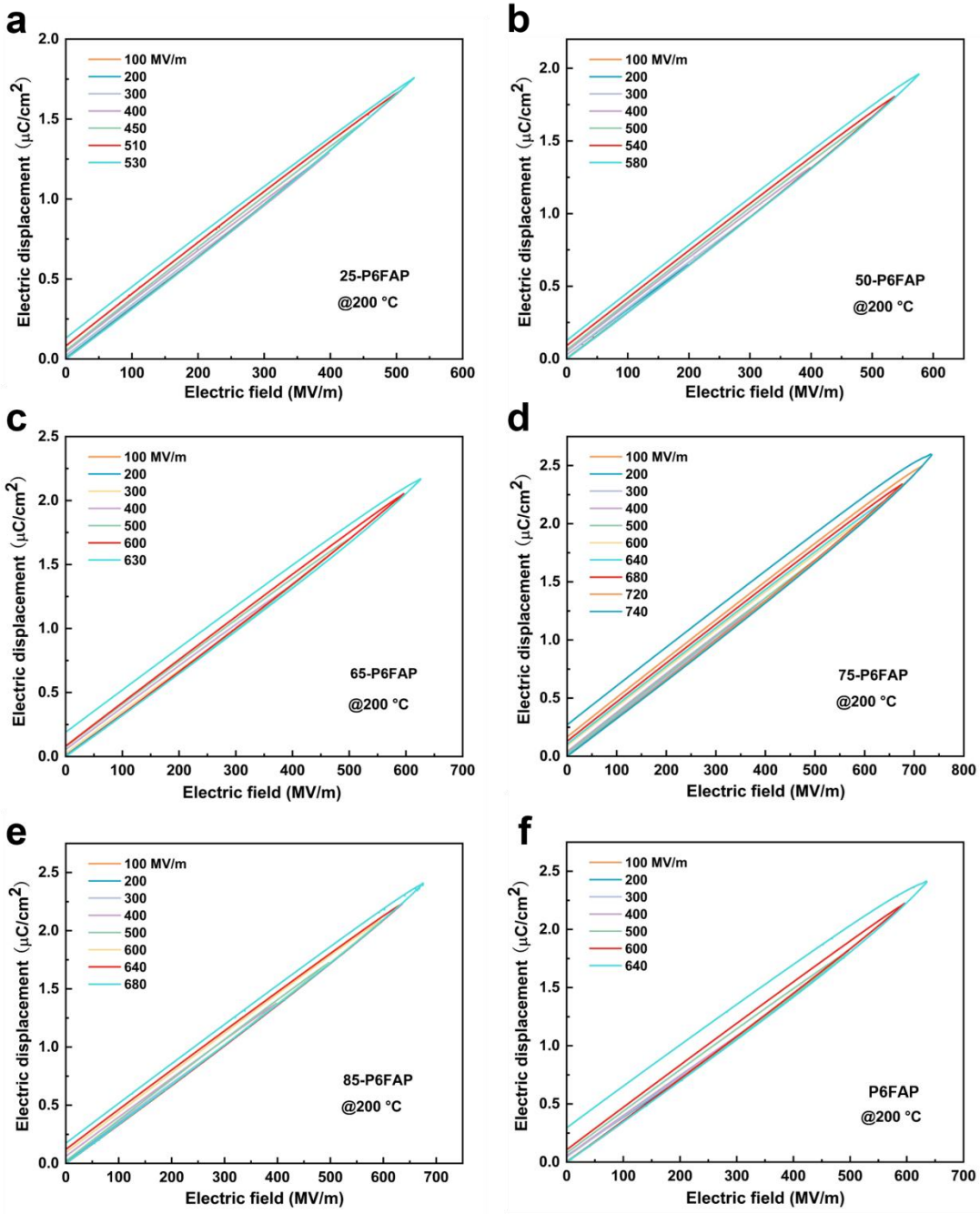

Fig. S14 Unipolar *D-E* loops of P6FAP dielectrics with different mole fractions of 6FAP diamine monomer at 200 °C.

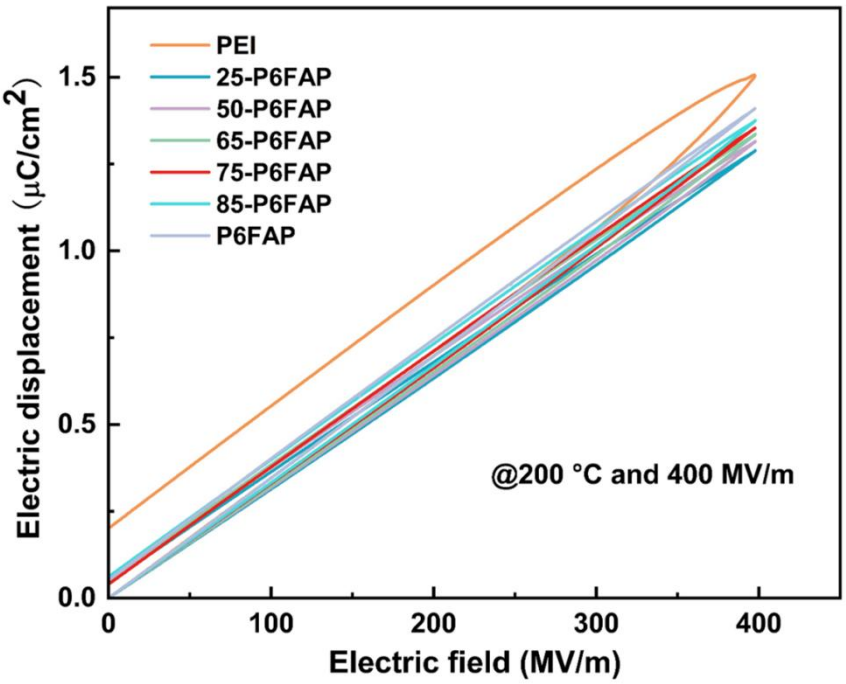

Fig. S15 Comparison of the unipolar *D-E* loops of pristine PEI and P6FAP dielectrics with different mole fractions of 6FAP diamine monomer at 200 °C and 400 MV/m.

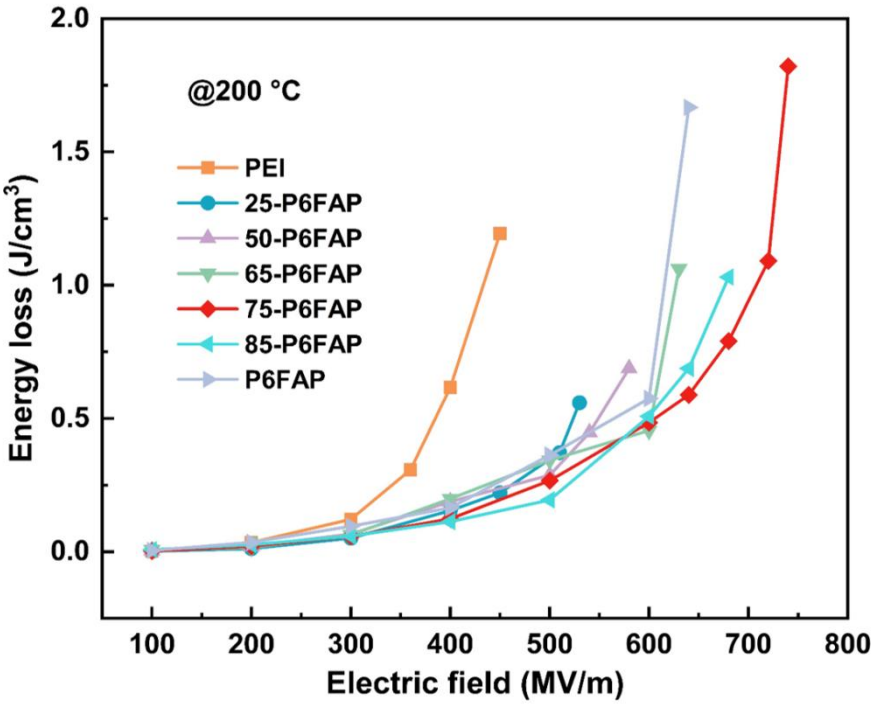

Fig. S16 Energy loss of pristine PEI and P6FAP dielectrics with different mole fractions of 6FAP diamine monomer at 200 °C and 400 MV/m.

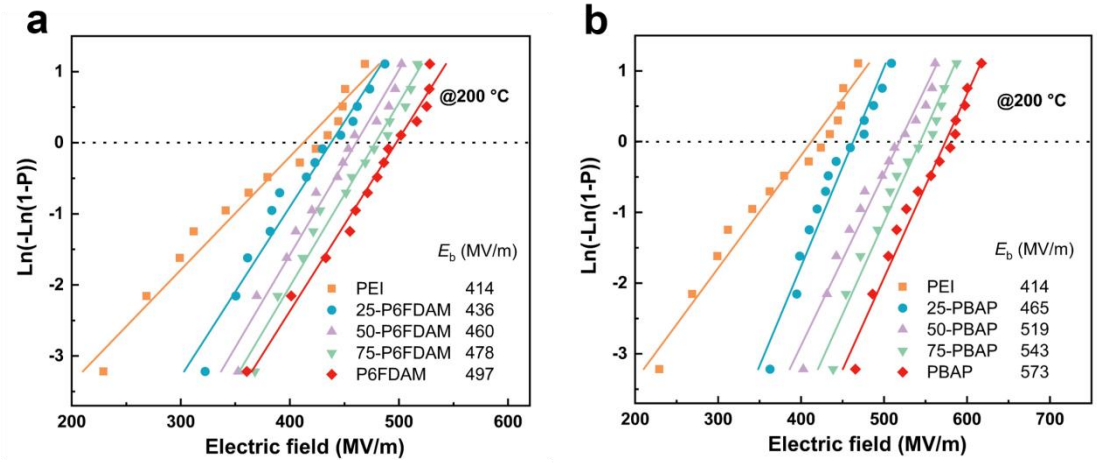

Fig. S17 a Weibull distribution of breakdown strength of pristine PEI and P6FDAM dielectrics with different mole fractions of 6FDAM diamine monomer at 200 °C. **b** Weibull distribution of breakdown strength of pristine PEI and PBAP dielectrics with different mole fractions of BAP diamine monomer at 200 °C.

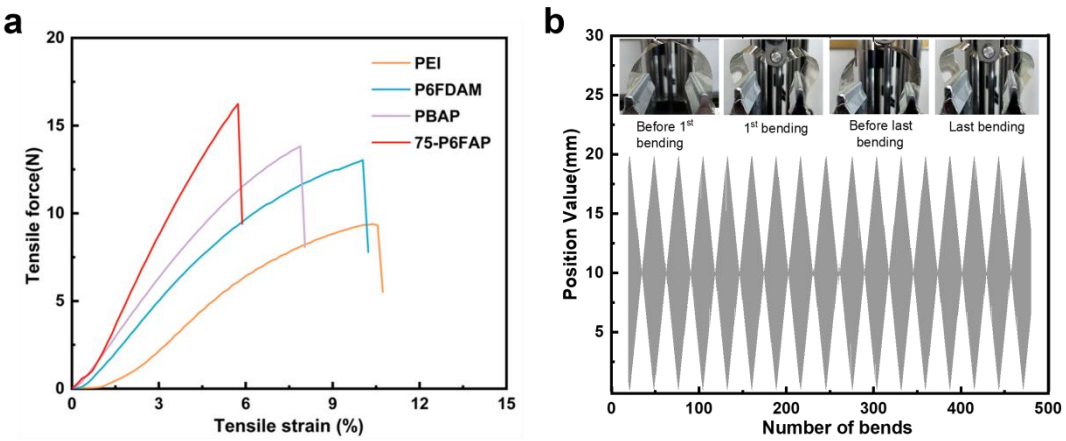

Fig. S18 a Stress-strain curves of various polymers. **b** Bending cycles of 75-P6FAP copolymer.

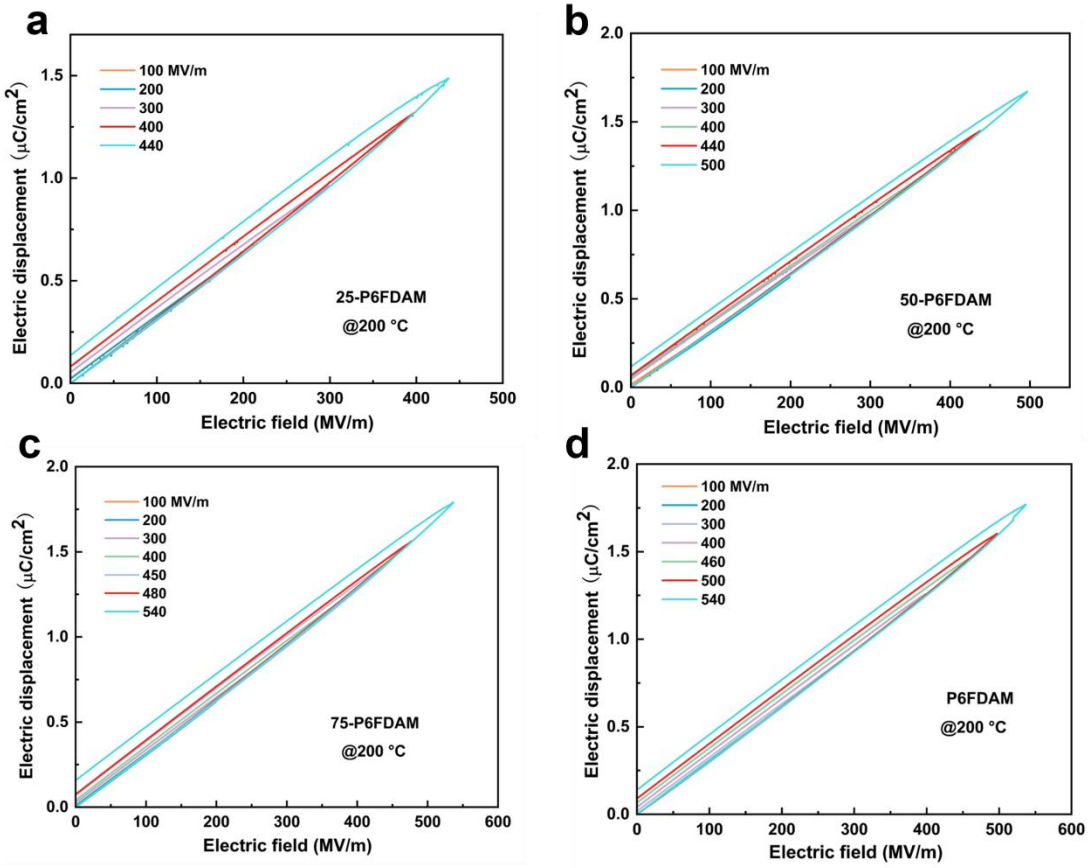

Fig. S19 Unipolar *D-E* loops of P6FDAM dielectrics with different mole fractions of 6FDAM diamine monomer at 200 °C.

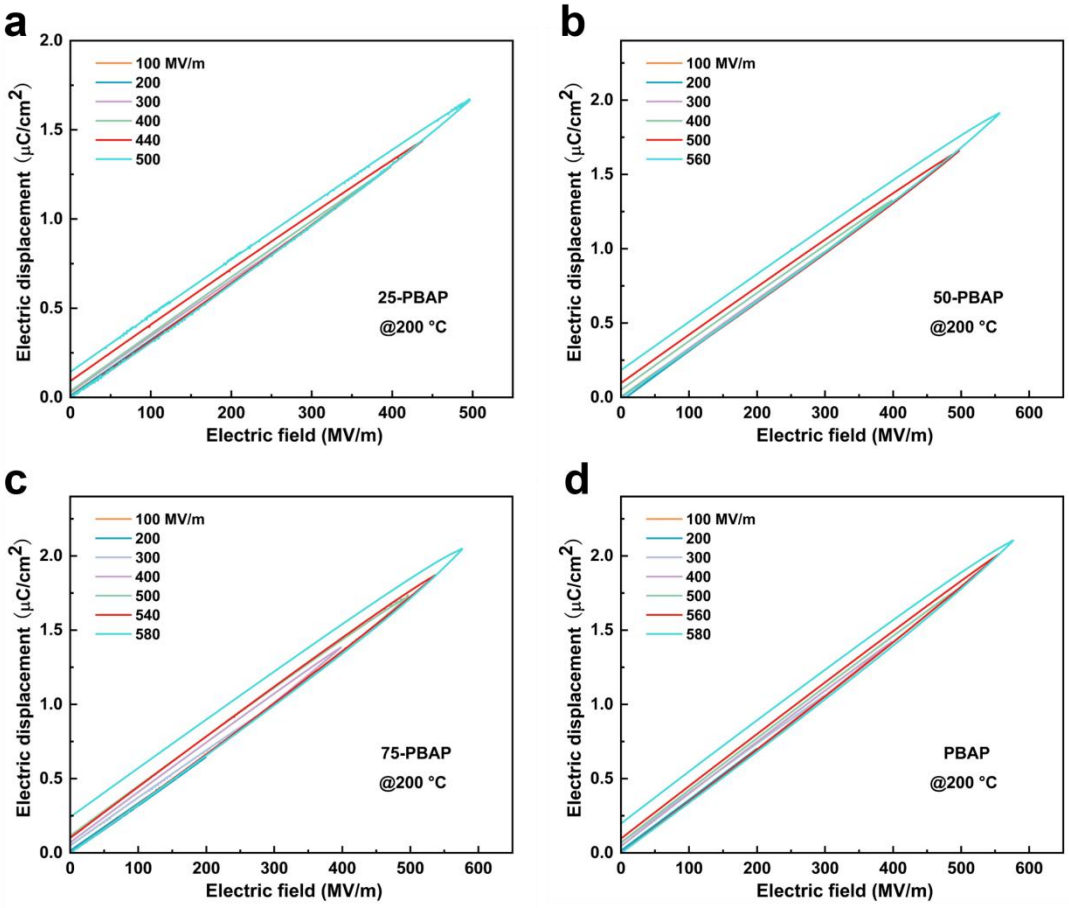

Fig. S20 Unipolar *D-E* loops of PBAP dielectrics with different mole fractions of BAP diamine monomer at 200 °C.

Table. S1 GPC results for various polymers

Samples	M_n (×10^4 g/mol)	M_w (×10^4 g/mol)	PDI
PEI	20.15	80.11	3.97
P6FDAM	16.05	42.82	2.66
PBAP	13.40	38.16	2.84
P6FAP	5.10	16.00	3.13
75-P6FAP	5.11	17.63	3.45

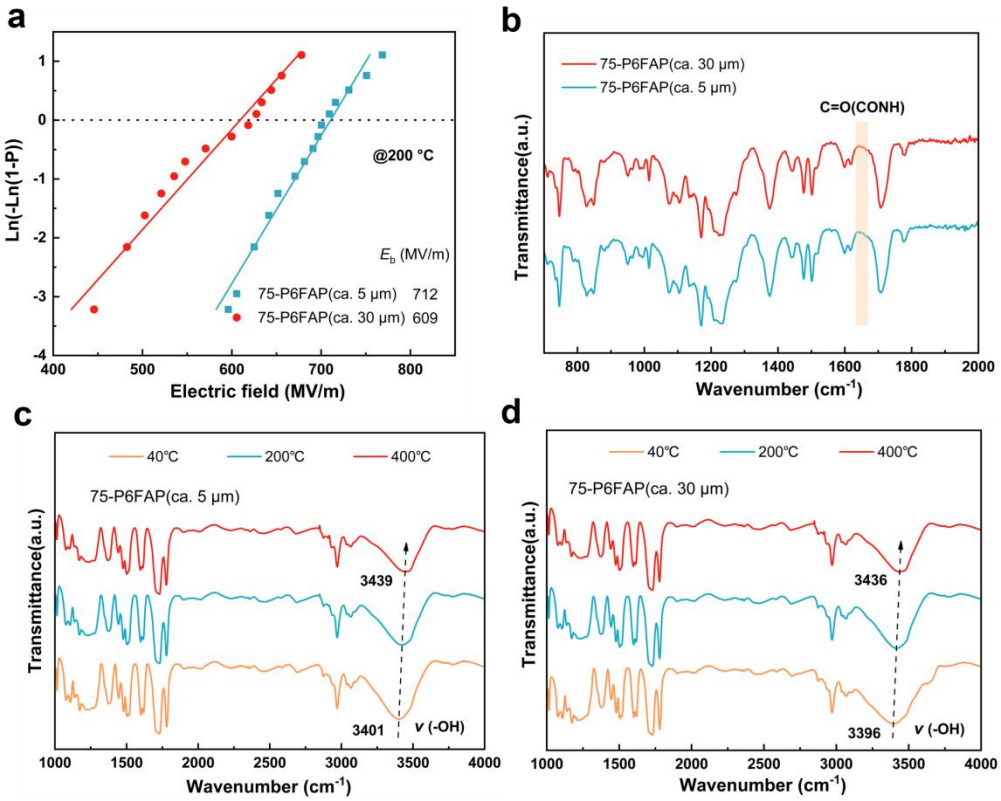

Fig. S21 **a** Weibull distribution of breakdown strength and **b** FT-IR spectra of 75-P6FAP copolymer films with different thicknesses. VT-IR spectra of the 75-P6FAP copolymer **c** thinner and **d** thicker films.

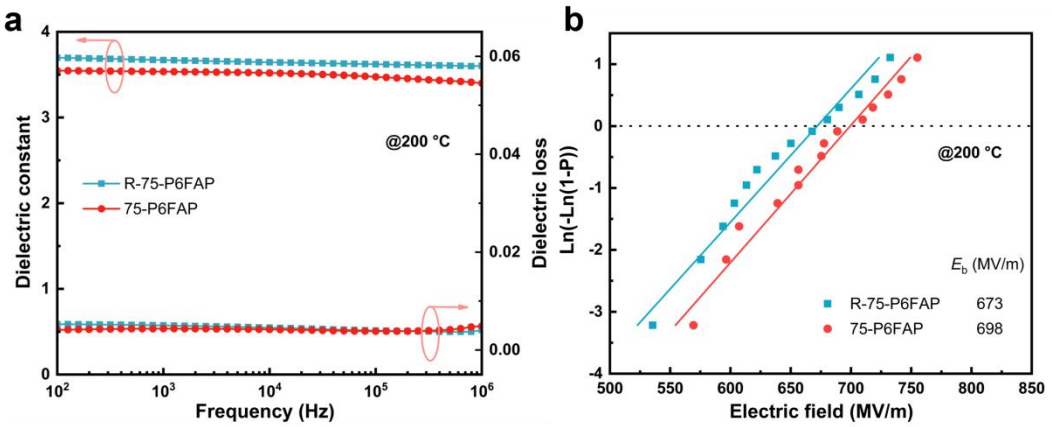

Fig. S22 Comparison of the dielectric properties and breakdown strength of 75-P6FAP copolymer before and after reprocessing.

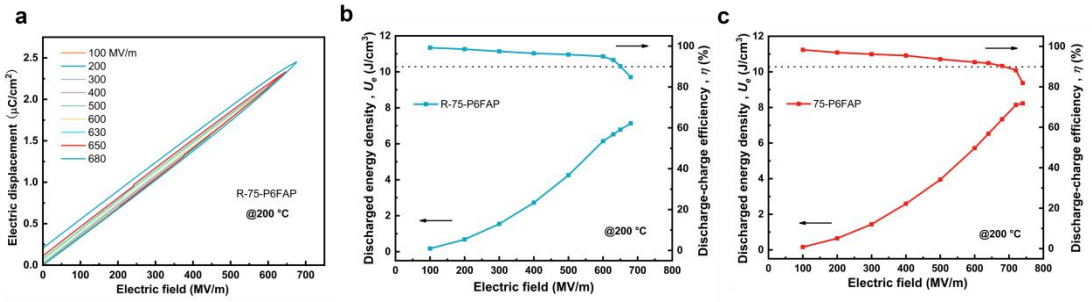

Fig. S23 Comparison of the high-temperature capacitive energy storage performance of 75-P6FAP copolymer before and after reprocessing.

References

1. Yang, M. *et al.* Surface ion-activated polymer composite dielectrics for superior high-temperature capacitive energy storage. *Energy Environ. Sci.* **17**, 1592-1602 (2024).

2. Yang, M. *et al.* Unifying and suppressing conduction losses of polymer dielectrics for superior high-temperature capacitive energy storage. *Adv. Mater.* **36**, 2309640 (2024).

3. Chiu, F.-C. A review on conduction mechanisms in dielectric films. *Advances in Materials Science and Engineering* **2014** (2014).